Modelling the lagged impacts of hourly weather and speed variation factors on the segment crash risk of rural interstate freeways: Applying a space-time-stratified case-crossover design

Zihang Wei*
Ph.D. Student
Zachry Department of Civil & Environmental Engineering
Texas A&M University
3136 TAMU, College Station, TX 77843-3136
Email: wzh96@tamu.edu

Subasish Das, Ph.D.
Assistant Professor
Ingram School of Engineering
Texas State University
601 University Dr, San Marcos, TX 78666
Email: subasish@txstate.edu

Yue Wu
Graduate Student
Zachry Department of Civil & Environmental Engineering
Texas A&M University
3136 TAMU, College Station, TX 77843-3136
Email: wywy@tamu.edu

Zihao Li
Ph.D. Student
Zachry Department of Civil & Environmental Engineering
Texas A&M University
3136 TAMU, College Station, TX 77843-3136
Email: scottlzh@tamu.edu

Yunlong Zhang, Ph.D.
Professor
Zachry Department of Civil & Environmental Engineering
Texas A&M University
3136 TAMU, College Station, TX 77843-3136
Email: yzhang@civil.tamu.edu

*** Corresponding Author**

Modelling the lagged impacts of hourly weather and speed variation factors on the segment crash risk of rural interstate freeways: Applying a space-time-stratified case-crossover design

ABSTRACT

Weather and speed variation factors are closely related to the crash risk of a roadway segment. These time-varying factors may impact segment crash risk not only at the time when a crash occurs but also during a certain time period afterwards. Previous studies always utilize data with large aggregation intervals (e.g., monthly and daily) to analyze the impact of these factors on segment crash risk. Since the resolutions of daily and monthly aggregation intervals are very coarse, this makes it impossible to investigate the lagged impacts of these factors on segment crash risk. In this study, hourly crash data on rural interstate highways in Texas, United States is used to investigate the lagged impacts on segment crash risk of four hourly time-series variables of precipitation, visibility, speed standard deviation, and temperature. The lagged impact is also termed as exposure-lag-response association in this study. A distributed lag model (DLM) and a distributed lag non-linear model (DLNM) are applied to model the exposure-lag response association. The results show that for these four time-series variables, the hourly lagged impacts on the crash risk of a roadway segment exist and have different exposure-lag response association patterns during the lagged hours. Moreover, compared with the results by DLM, DLNM can provide more information on the hourly lagged impacts on segment crash risk due to precipitation and temperature.

Keywords: Weather factors, Hourly crash data, Exposure-lag response association*, Distributed lag model, Distributed lag non-linear model, Rural interstate.*

INTRODUCTION

Roadway traffic crashes are one of the major factors that cause deaths and financial losses. In the United States, an estimated number of 42,915 people died in motor vehicle traffic crashes in 2021, representing a 10.5% increase from about 38,824 fatalities in 2020 and is the highest fatality number since 2005. Among these, there are about 2,147 fatalities on rural interstate in 2021 which is a 15% increase from 2021 (National Center for Statistics and Analysis, 2022). Roadway geometry (Anderson et al., 1999; Haghighi et al., 2018; Miaou and Lum, 1993), speed distribution (Garber and Gadiraju, 1989; Lee et al., 2002; Pei et al., 2012; Wang et al., 2018), and weather conditions (Brijs et al., 2008; Eisenberg, 2004; Jaroszweski and McNamara, 2014; Scott, 1986; Yu and Abdel-Aty, 2014) are considered to be closely related to the crash risk of a roadway segment. There is a need for researchers and policymakers to gain a better understanding of what factors potentially increase segment crash risk and in what ways does these factors increase segment crash risk.

The modeling of previous studies often assumed that weather condition and speed variation events only affect the crash risk of a roadway segment during the period when the crashes happen. However, one important question remains to be answered: whether there are also lagged impacts on segment crash risk brough by server weather condition or high speed variations? Precipitation is found to have a lagged impact on roadway crash risk (Eisenberg, 2004). This phenomenon is related to engine-oil and gasoline accumulated on roadway surface under dry condition. After precipitation happens, it takes some time for accumulated rainfall to be mixed with the engine-oil and gasoline on the roadway surface, making the roadway surface slippery a while after precipitation happens. Thus, it is reasonable to believe that other weather condition factors and speed variation factors may also have lagged impacts on segment crash risk.

Traditional crash models usually use data with large aggregation interval. For example, the effect of roadway geometry on roadway crash risk has been widely investigated using yearly or monthly aggregated crash data. Some studies have investigated the impact of weather condition factors on roadway crash risk, usually using daily aggregated data for analysis. However, since weather conditions and speed variations are highly time-varying (Lord and Mannering, 2010; Pei et al., 2012; Wang et al., 2018). In order to investigate the lagged impacts of these factors on segment crash risk, data need to be aggregated into smaller interval to better capture the time-varying nature. As a result, this study aggregates data using an hourly interval.

To the authors' best knowledge, no related studies have investigated the lagged impacts of hourly precipitation, hourly visibility, hourly temperature, and hourly speed standard deviation on the crash risk of a roadway segment. This study aims to bridge this research gap. In this study, the lagged impacts of weather condition and speed variations on segment crash risk are investigated using hourly aggregated data on rural interstate highways in Texas. This lagged effect is also termed as exposure-lag-response association (Gasparrini, 2014). Four time-series variables, hourly precipitation, hourly visibility, hourly speed standard deviation, and hourly temperature, are considered.

LITERATURE REVIEW

Gaining a better understanding of the factors that influence the crash risk of a roadway segment has long been a research focus. The effects of weather conditions, and vehicle speed distribution

were widely examined in previous studies. Scott (1986) selected temperature and precipitation as explanatory variables to model the time-series crash data. In the study, single-vehicle crashes were modeled using a regression model, and two-vehicle crashes were modeled using a Box-Jenkins model. Eisenberg (2004) used negative binomial regression analysis to study the effect of monthly and daily precipitation on fatal crash rates. It is found that there was a significant inverse correlation between fatal crash frequency and precipitation at a monthly level, but a significant positive correlation between fatal crash frequency and precipitation at a daily level. Brijs et al. (2008) proposed an integer autoregressive model to model crash occurrence with time-dependent nature using daily crash data. Their results indicated a significant correlation between rainfall intensity and daily crash count. Yu and Abdel-Aty (2014) developed a crash injury severity analysis model for a mountainous freeway section to study the relationship between crash severity and weather conditions. They found that snowy weather decreased the chance of severe crashes, while lower temperatures increased the chance of severe crashes on mountainous freeways. Andrey and Yagar (1993) used a matched sample approach to analyze the relationship between rainfall and crash risk using hourly precipitation data. Moreover, Omranian et al. (2018) applied a matched-pairs analysis approach to investigate the effect of precipitation on roadway crash risk in Texas using hourly level data.

Studies also considered speed distribution as a critical factor of roadway crash risk (Das et al., 2022a, 2022b, 2021, 2020; Das and White, 2020; McCourt et al., 2019; Park et al., 2021). Garber and Gadiraju (1989) examined the effect of mean speed and speed variation on crash rates. According to their findings, while an increase in mean speed does not always result in a higher crash rate, a higher speed variance can. Lee et al. (2002) developed an aggregated log-linear model to predict crash occurrence by utilizing real-time traffic flow data from loop detectors and concluded that traffic density and speed variation are significant predictors of crash frequency. Pei et al. (2012) used disaggregated speed and crash data with a 4-hour interval during various times of the day to investigate the correlation between mean speed and crash occurrence. They revealed that the mean speed and crash frequency have a positive relationship when exposure to distance is considered, but a negative relationship when exposure to time is considered. Wang et al. (2018) modeled crash frequency using a hierarchical Poisson log-normal (HPLN) model to analyze the relationship between mean speed, speed variation, and crash frequency on arterials in urban areas. Considering that speed distribution tends to fluctuate through the day, the study aggregated crash data into three study periods (morning, midday, and evening), each of which was three hours long. They found that higher average speeds and higher speed variations on urban arterial roads result in higher crash frequency.

Some studies also analyzed the collaborative effect of different factors on roadway crash risk (Dutta and Fontaine, 2019; Shankar et al., 1995). Wei et al. (2022a) combined weather, speed distribution, and roadway geometric-related variables to investigate their impacts on daily crash occurrences in rural two-lane roadways. For weather conditions' impact on roadway crash risk, previous studies have tended to use daily aggregation intervals for crash data preparation. Das et al. (2022a) developed a real-time roadway safety decision tool considering roadway geometry, weather condition, and speed distribution to improve rural roadway safety.

Weather-related events are considered to have lasting effects on roadway safety. For example, changes in segment crash risk brought by precipitation may exist for a period after it happened.

Traditional methods tend to assume that crashes are only related to events that happens during the same period and ignore the events' lagged impacts. Some studies attempted to study the lagged impact of weather factors on crash risk. Xing et al. (2019) investigated the lag effects of the association between weather factors and crashes using an integrated meteorological, traffic, and crash dataset in Hong Kong. Temperature, humidity, rain intensity, and wind speed data were used at 1-hour interval. Zhan et al. (2020) examined the lagged effects of hourly temperature and hourly precipitation on road traffic casualty in the city of Shenzhen, China using roadway traffic casualty data. The data used by Xing et al. (2019) and Zhan et al. (2020) is the hourly total of crashes in the entire city. However, for evaluating crash risks, it is better to summarize the hourly total of crashes on each roadway segment in order to provide high-resolution information on identifying the roadway segments with higher crash risks. The main contribution of our study is that this is the first one to consider the lagged impacts of weather condition and speed variation of short duration crash risk using roadway segment level data.

DATA PREPARATION

The data preparation process contains three steps. The data preparation process is illustrated in the following flow chart (**Figure 1**). Details on the data are provided after the flowchart.

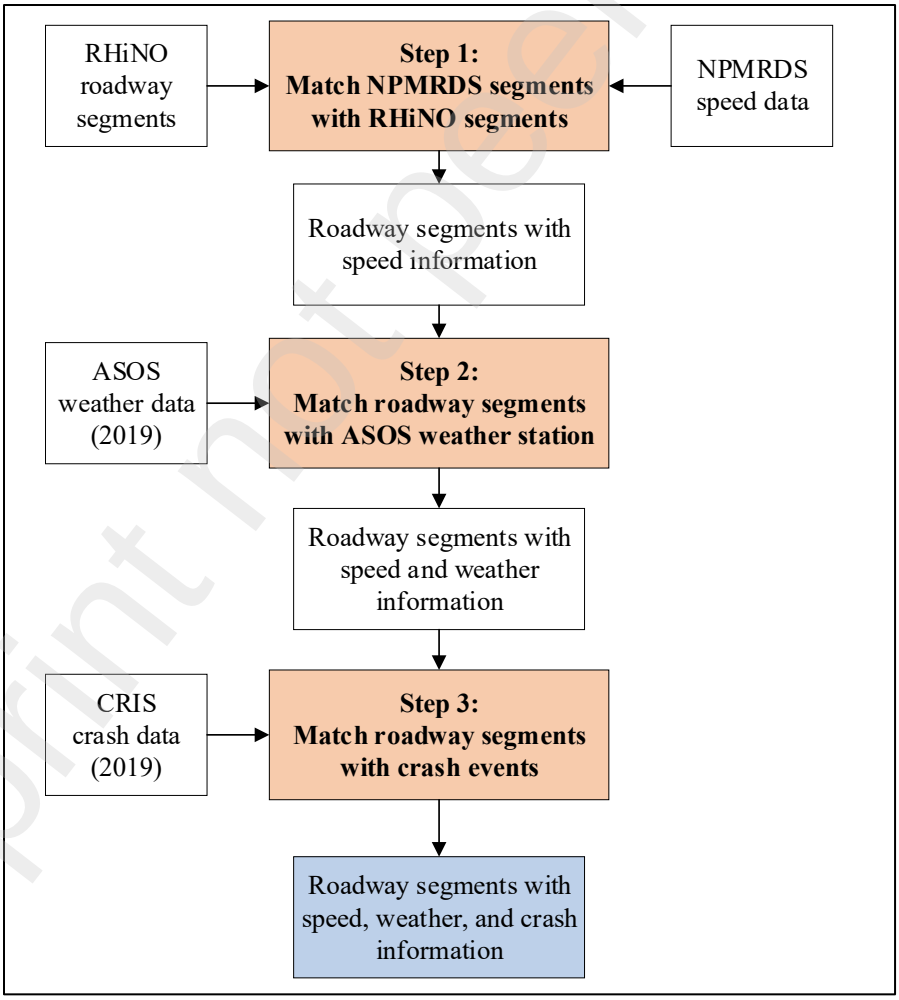

Figure 1. Flow chart of the data preparation process.

Base Roadway Segment

The base roadway segment network consists of rural interstate highways in the State of Texas. The data was collected from the Texas Department of Transportation (TxDOT) Road-Highway Inventory Network Offload (RHiNO), which contains roadway GIS linework and roadway inventory attributes, including geometric features and traffic information. TxDOT submitted this dataset to the Federal Highway Administration (FHWA) as part of the Highway Performance Monitoring System (HPMS) program (Texas Department of Transportation, 2020). In this study, all rural interstate roadway segments from RHiNO are included in the analysis.

Speed Distribution Data

Raw speed data are collected from FHWA's National Performance Management Research Dataset (NPMRDS). The NPMRDS contains travel time and speed data collected from a fleet of probe vehicles (e.g., cars and trucks). The NPMRDS can generate speed and travel time data using probe vehicle location information. Speed data are collected based on traffic message channels (TMC). TMC segments and base roadway network segments can be matched with each other using GIS software. This study calculated the hourly speed standard deviation using the raw speed data, which is collected in a 5-minute interval.

Weather Condition Data

Weather condition data are collected from the Automated Surface Observing System (ASOS) of the National Centers for Environmental Information (NOAA). This study utilized all the ASOS stations in Texas, and each base roadway segment is assigned to the ASOS station closest to it. A 30 miles buffer is applied when assigning ASOS weather stations to roadway segments. This ensures that the ASOS station assigned to each roadway segment is less than 30 miles away, which means the weather information collected at the assigned ASOS station can almost accurately reflect the weather condition of the roadway segment. Weather information, including precipitation, visibility, and temperature, was collected for each weather station, and it is averaged into one-hour intervals.

Crash Data

Crash data are collected within the state of Texas in 2019 through the Crash Record Information System (CRIS). Each crash record includes location and date information. Through GIS software, all crashes are assigned to the base roadway segments on which they occurred. The hourly crash number is summarized for each roadway segment. This study uses the total number of crashes that occurred on a roadway segment in 1 hour to represent the hourly roadway crash risk. This is to say, in the modeling process, the hourly crash number of a roadway segment is used as the dependent variable.

Space-time-stratified case-crossover design

Due to the rare nature of crash events, there are a significantly larger number of non-crash hours than crash hours after crash data are aggregated at hourly level. In order to achieve more accurate results, a space-time-stratified case-crossover design is applied to restructure the data. This approach is widely used in epidemiology and environmental health-related research (Gao et al., 2022; Guo et al., 2011; Nyadanu et al., 2022; Wu et al., 2021). The design compares an hourly observation where crashes happened (case hour) with hourly observations where no crash happened (control hours) while controlling the space (e.g., roadway segment) and time (e.g., hour) factors. The control hours are served as the counterfactual exposure experience of each

case hour. For each case hour, a stratum ID combining space and time dimensions is introduced and more specifically, a case hour is matched with control hours on the same roadway segment at the same hour on the same day of week in the same month. Usually, a case hour is matched with 3 or 4 control hours on the same day of week in the same month (see **Table 1**). This design can control the impact of roadway geometry factors on segment crash risk and additionally, it can also control the impact of the time of week, time of day and seasonality on segment crash risk. In this study, stratum ID is the combination of road ID, year, month, day of week, and hour (see **Table 1**). For each case hour, all its control hours are also included in the case-crossover dataset.

Table 1. Space-Time-Stratified Case-Crossover Design

Road ID	year	month	day	hour	Day of Week	Total Crash	Stratum ID	Case / Control
1000	**2019**	**1**	**2**	**14**	**4**	**1**	**1000 2019 1 4 14**	**Case**
1000	2019	1	9	14	4	0	1000 2019 1 4 14	Control
1000	2019	1	16	14	4	0	1000 2019 1 4 14	Control
1000	2019	1	23	14	4	0	1000 2019 1 4 14	Control
1000	2019	1	30	14	4	0	1000 2019 1 4 14	Control
1001	**2019**	**12**	**24**	**22**	**3**	**2**	**1001 2019 12 3 22**	**Case**
1001	2019	12	3	22	3	0	1001 2019 12 3 22	Control
1001	2019	12	10	22	3	0	1001 2019 12 3 22	Control
1001	2019	12	17	22	3	0	1001 2019 12 3 22	Control

Note: lines in bold text are case hours

Time series variables

In order to investigate the lagged impact of hourly Precipitation, hourly visibility, hourly temperature, and hourly speed standard deviation on segment crash risk, these variables are considered as time-series variables in this study because on one roadway segment, the crash occurrence within one specific hour is not necessarily related to the exposure in the same hour but potentially related to the exposure in the preceding hours. The exposures happened in the preceding hours have lagged impact on segment crash risk in the current hour. Thus, during the modeling process, the models should consider the exposure at the current hour when crashes occur and the exposure at the preceding hours before crashes occur as well. Based on the modeling results, the analysis in this study considers hourly precipitation for 8 preceding hours and considers hourly visibility, hourly temperature, and hourly speed standard deviation for 10 preceding hours.

Table 2 presents the descriptive statistics of all time-series variables at the current hour and each preceding hour separately for case hours and control hours. As shown by the table, the descriptive statistics show that time-series variables may have lagged impact on segment crash risk. For example, for hourly precipitation, the average hourly precipitation at the immediate preceding hour of the case hour is 0.0111 inches which are more than 2 times larger than the average hourly precipitation at the current hour (i.e., 0.0045 inches). Moreover, the averages of hourly precipitation at the 3rd to 6th preceding hours are also larger than that of the current hour. While as for the control hours, averages of hourly precipitation at the current hour and each preceding hour are all around 0.003 inches. This indicates that crashes that happen at the case

hours are linked to the lagged impact brought by high precipitation exposures at the preceding hours. For hourly speed standard deviation, the average hourly speed standard deviation at the case hours is the highest (e.g., 5.5 mph), and the value decreases at each preceding hour (e.g., 4.1 mph at the immediate preceding hour, 3.8 mph at the 2nd preceding hour). While for the control hours, the averages of hourly speed standard deviation at the current hour and each preceding hour are all around 3.5 mph.

Table 2. Descriptive Statistics of variables at the current hour and each preceding hour

Variables	Mean	Std.	Min	Max	Variables	Mean	Std.	Min	Max
Case hours (Number of crashes > 0)					***Control hours (Number of crashes = 0)***				
Hourly precipitation (inches)					**Hourly precipitation (inches)**				
Current hour	0.0045	0.0423	0	2	Current hour	0.0029	0.0383	0	2
Preceding hour 1	0.0111	0.3251	0	17	Preceding hour 1	0.003	0.0375	0	2
Preceding hour 2	0.0044	0.0388	0	1	Preceding hour 2	0.0034	0.1076	0	17
Preceding hour 3	0.0058	0.0648	0	2	Preceding hour 3	0.003	0.0376	0	2
Preceding hour 4	0.0074	0.2701	0	24	Preceding hour 4	0.0039	0.1484	0	17
Preceding hour 5	0.0162	0.5184	0	24	Preceding hour 5	0.0028	0.0366	0	2
Preceding hour 6	0.0094	0.2698	0	21	Preceding hour 6	0.0039	0.1515	0	24
Preceding hour 7	0.0039	0.0401	0	1	Preceding hour 7	0.0029	0.054	0	7
Preceding hour 8	0.0039	0.0426	0	1	Preceding hour 8	0.0043	0.2095	0	24
Hourly visibility (miles)					**Hourly visibility (miles)**				
Current hour	9.0020	2.2296	0	10	Current hour	9.1791	2.0383	0	10
Preceding hour 1	9.0029	2.2182	0	10	Preceding hour 1	9.1434	2.0833	0	10
Preceding hour 2	9.0330	2.1684	0	10	Preceding hour 2	9.1243	2.1127	0	10
Preceding hour 3	9.0328	2.1732	0	10	Preceding hour 3	9.1183	2.1112	0	10
Preceding hour 4	9.0396	2.1657	0	10	Preceding hour 4	9.1167	2.1164	0	10
Preceding hour 5	9.0629	2.1605	0	10	Preceding hour 5	9.1254	2.1026	0	10
Preceding hour 6	9.1048	2.1102	0	10	Preceding hour 6	9.1531	2.0673	0	10
Preceding hour 7	9.1318	2.0964	0	10	Preceding hour 7	9.1935	2.011	0	10
Preceding hour 8	9.1706	2.0503	0	10	Preceding hour 8	9.2399	1.9553	0	10
Preceding hour 9	9.2154	2.0088	0	10	Preceding hour 9	9.2764	1.9097	0	10
Preceding hour 10	9.2471	1.9649	0	10	Preceding hour 10	9.3157	1.8607	0	10
Hourly temperature (°F)					**Hourly temperature (°F)**				
Current hour	67.1679	17.2751	11	106	Current hour	67.279	17.2585	9	109
Preceding hour 1	66.6303	17.0922	9	104	Preceding hour 1	66.6909	17.1131	11	106
Preceding hour 2	66.1092	16.9440	8	103	Preceding hour 2	66.1792	16.9455	9	106
Preceding hour 3	65.6871	16.7986	9	104	Preceding hour 3	65.7378	16.7697	9	108
Preceding hour 4	65.4004	16.6734	9	105	Preceding hour 4	65.4493	16.6168	10	109
Preceding hour 5	65.2642	16.5773	10	106	Preceding hour 5	65.3159	16.5207	9	108
Preceding hour 6	65.3091	16.5472	10	105	Preceding hour 6	65.3399	16.4985	9	107
Preceding hour 7	65.5452	16.5650	10	105	Preceding hour 7	65.5709	16.523	9	108
Preceding hour 8	65.8580	16.6578	10	106	Preceding hour 8	65.9167	16.5632	9	108
Preceding hour 9	66.2151	16.7300	11	106	Preceding hour 9	66.3141	16.6109	10	108
Preceding hour 10	66.7053	16.8420	12	106	Preceding hour 10	66.8024	16.6606	10	108
Hourly speed standard deviation (mph)					**Hourly speed standard deviation (mph)**				
Current hour	5.5483	3.6371	0	28	Current hour	3.5568	1.8205	0	28
Preceding hour 1	4.0843	2.3973	0	23	Preceding hour 1	3.5554	1.7585	0	27
Preceding hour 2	3.7983	2.0703	0	24	Preceding hour 2	3.5397	1.7669	0	26
Preceding hour 3	3.7003	1.9014	0	21	Preceding hour 3	3.5369	1.7569	0	35
Preceding hour 4	3.6643	1.8909	0	24	Preceding hour 4	3.5293	1.7129	0	24
Preceding hour 5	3.6461	1.7913	0	19	Preceding hour 5	3.5265	1.7019	0	23
Preceding hour 6	3.6519	1.7534	0	19	Preceding hour 6	3.5349	1.6673	0	28
Preceding hour 7	3.6177	1.7486	0	23	Preceding hour 7	3.5573	1.6867	0	26
Preceding hour 8	3.6106	1.6678	0	23	Preceding hour 8	3.5704	1.6973	0	29
Preceding hour 9	3.6369	1.6641	0	19	Preceding hour 9	3.5829	1.667	0	29

Preceding hour 10	3.6348	1.6906	0	24	Preceding hour 10	3.6036	1.653	0	27

METHODOLOGY

This study applies two models, namely the distributed lag model (DLM) and the distributed lag nonlinear model (DLNM), to explore the exposure-lag-response relationship between four time-series variables and segment crash risk. Time-series variables include hourly precipitation, hourly visibility, hourly temperature, and hourly speed standard deviation. The segment crash risk is represented by the number of crashes that occurred on a roadway segment during a 1-hour period. The DLM model was first applied to investigate the lagged health effect of air pollution and temperature factors (Ferreira Braga et al., 2001; Schwartz, 2000; Zanobetti et al., 2000). Besides, the DLNM model is an improvement of the DLM model, which was first proposed by Gasparrini et al. (2010). The DLM model applies non-linear transformation on the lag space to form new variables which each is a weighted sum of the exposure variables at each lag time step. The DLNM model not only applies non-linear transformation to the lag space but also applies non-linear transformation to the exposure space. By doing so, the DLNM model can consider both the magnitude and the temporal effect of the exposures on the outcomes. The mathematical representations of the DLM and DLNM models are presented in the following sections.

Model Descriptions

Representation of the model design

The representation of the model design used in this study can be written as **Eq. (1)**:

$$f(\mu_t) = \alpha + \sum_{j}^{J} \sum_{i=1}^{N_j} \eta_i^j s_i^j(x,t) \quad (1)$$

Where $t = 1, \dots, n$ is the time index of the event, $\mu_t \equiv E(Y_t)$ is the expectation of the time series outcome Y_t, and f is a monotonic link function which assumes that Y_t comes from a distribution belonging to the exponential family. α is the model intercept. J is the set of time-series variables. $s_i^j(\cdot)$ is called the basis function of time-series variable j and N_j is the total number of basis functions applied to the lag space and exposure space of time-series variable j. η_i^j is the parameter of the variable created by the transformation $s_i^j(\cdot)$. N_j equals to v_l for DLM and equals to $v_l v_x$ for DLNM. This will be explained in the following sections. Based on the choices of the basis function $s_i^j(\cdot)$, the model is a DLM model if non-linear transformation is applied to the lag space and a DLNM model if non-linear transformation is applied to both the lag space and the exposure space. Detailed mathematical formulations will be explained in the following sections.

The basis function of DLM

For DLM, one basis function $s_i(x,t)$ of a time series variable can be written as **Eq. (2a) to (2c)**:

$$s_i(x,t) = \int_{t_0}^{t_1} x_u \, w_i(t-u) du \quad (2a)$$

$$= \int_{l_0}^{L} x_{t-l}\, w_i(l) dl \tag{2b}$$

$$\approx \sum_{l=l_0}^{L} x_{t-l} w_i(l) \tag{2c}$$

$$where\ i = 1, \dots, v_l$$

In **Eq. (2a)**, the risk at time t can be defined as the integral of exposure magnitude x_u over the time period from t_0 to t_1. Here, t_0 and t_1 are the first and last lag exposure times that are relevant to the risk at time t. $w_i(\cdot)$ is one weight function of the lag space. There is a total of v_l weight functions of the lag space where v_l is defined by the dimension of the transformation basis functions on the lag space. $w_i(t-u)$ can be viewed as the relative contribution of lag exposure at time $t-u$ on the risk at time t. $w_i(\cdot)$ can also be called the lag-response function. **Eq. (2a)** can be written as **Eq. (2b)**, where L is the total length of the lag period that has contributed to the risk at time t. l_0 is the start of the lag period, and it usually equals 0. Moreover, since real-life data are always discrete, **Eq. (2b)** can be estimated as **Eq. (2c)** where the lag interval is partitioned into discrete units, and the integral is estimated as the summation of all the discrete units. This method allows the effects of an exposure event to be distributed over a specific lag period defined by L and $s_i(x,t)$ can be viewed as a part of the cumulative impact at time t of an exposure event within lag time period L.

The simplest form of the DLM model is called the unconstrained DLM, which simply includes a parameter at each time lag (Schwartz, 2000). However, doing so will result in the model having high level of collinearity since the exposures in adjacent time lags are closely related to each other, which will result in poor model performance. By applying some constraints to the parameters at each time lag, it is possible to improve the model's performance. For example, Schwartz (2000) applied polynomial functions to constrain the parameters at each time lag. Zanobetti et al. (2000) applied spline functions to constrain the parameters.

By using matrix notation, it is possible to write **Eq. (2)** in a more compact form as follows:

$$s(x,t,\eta) = q_{x,t}^T C\eta = w_{x,t}^T \eta \tag{3}$$

C is a matrix of shape $(L - l_0 + 1) \times v_l$ which is obtained by applying v_l basis functions to the lag vector $\delta = [l_0, l_1, \dots, L]^T$. $q_{x,t} = [x_{t-l_0}, x_{t-l_1}, \dots, x_{t-L}]^T$ which is the exposure history vector containing exposure values at each time lag within exposure period L. Note that in most cases, l_0 equals to 0. $w_{x,t}$ is now a vector of length v_l where each element is a weighted sum of all exposure history within lag period L. By stacking $w_{x,t}^T$ row wise, we can get a matrix W which can also be derived by **Eq. (4)**:

$$W = QC \tag{4}$$

Where W is a matrix of the shape $N \times v_l$ and Q is a matrix of shape $N \times (L - l_0 + 1)$ where N is the total number of observations. Note that here each row of matrix Q is the vector $q_{x,t}^T$ of a single observation, and each row of matrix W is $w_{x,t}^T$ of a single observation. The parameters η

corresponding to the v_l new variables can be estimated by including matrix W into the designed matrix. The original parameters $\hat{\beta}$ representing the risk contribution at each time lag and the corresponding (co)variance matrix $V(\hat{\beta})$ can be calculated after the estimated $\hat{\eta}$ is obtained:

$$\begin{aligned} \hat{\beta} &= C\hat{\eta} \\ V(\hat{\beta}) &= CV(\hat{\eta})C^T \end{aligned} \tag{5}$$

After obtaining $\hat{\beta}$ which is a vector of length $L - l_0 + 1$, each element $\hat{\beta}_l$ in $\hat{\beta}$ can be view as two ways. One is forward that one unit change of the exposure variable in the current time step will result in a $\hat{\beta}_l$ unit change of the risk after l time steps. The other is backward, which is to say that a $\hat{\beta}_l$ unit change of risk at the current time step is the result of one unit change of the exposure at l time steps early. With $\hat{\beta}$, it is possible to unveil the impact of an exposure event at the current time step on the changes of risk level during a period after the exposure event happens.

The basis function of DLNM

For DLNM, one basis function $s_{k,i}(x,t)$ of a time series variable can be written as **Eq. (6a) and (6b)**:

$$s_{k,i}(x,t) = \int_{l_0}^{L} f_k(x_{t-l})\, w_i(l) dl \tag{6a}$$

$$\approx \sum_{l=l_0}^{L} f_k(x_{t-l}) w_i(l) \tag{6b}$$

$$where\ k = 1, \dots, v_x\ and\ i = 1, \dots, v_l$$

In **Eq. (6a) and (6b)**, the definitions of v_l, L, and l_0 are the same as the definitions in **Eq. (2)**. Unlike DLM, there is a new weight function $f_k(\cdot)$ introduced in DLNM. This weight function is applied on the exposure space and there is a total of v_x weight functions and v_x is defined by the dimension of the transformation basis function on the exposure space. $f_k(\cdot)$ can also be called as the exposure-response function. The core ideas of DLM and DLNM are similar. However, DLM only applies transformation onto the lag space while DLNM not only applies transformation onto the lag space but also applies transformation onto the exposure space. The combination of the transformation basis functions of the lag space and exposure are called cross-basis functions and the core concept of DLNM is to apply the cross-basis functions to transform the time-series variables and their corresponding lags. In this case, there are a total of $v_x v_l$ cross-basis functions. The algebraic representations of the DLNM basis function are as following. Let $A_{x,t}$ equals to:

$$A_{x,t} = (1_{vl}^T \otimes R_{x,t}) \odot (C \otimes 1_{vx}^T) \tag{7}$$

$$s(x,t,\eta) = \left(1_{L-l_0+1}^T A_{x,t}\right)\eta = w_{x,t}^T \eta \tag{8}$$

$w_{x,t}$ is the vector of $v_x v_l$ new variables obtained by applying exposure-response function and lag response function to the exposure and lag space. Note that here $\otimes$ represent the Kronecker product and $\odot$ represent the Hadamard product. C is the same as **Eq. (3)**. $R_{x,t}$ is a matrix of shape $(L - l_0 + 1) \times v_x$ which is obtained by applying v_x basis functions to the exposure history vector $q_{x,t} = [x_{t-l_0}, x_{t-l_1}, \dots, x_{t-L}]^T$.

By stacking $w_{x,t}^T$ row wise, we can get a matrix W of the shape $N \times v_l v_x$. This matrix can be included into the design matrix to estimate parameters η corresponding to the $v_x v_l$ new variables. After obtaining the estimated variables $\hat{\eta}$. Parameters $\hat{\beta}_{x_p}$ representing the risk contribution during the $L - l_0 + 1$ lag period by exposure change and the corresponding (co)variance matrix $V\left(\hat{\beta}_{x_p}\right)$ can be calculated using a similar fashion as the DLM.

$$\begin{aligned} \hat{\beta}_{x_p} &= A_{x_p}\hat{\eta} \\ V\left(\hat{\beta}_{x_p}\right) &= A_{x_p} V(\hat{\eta}) {A_{x_p}}^T \end{aligned} \tag{9}$$

Note that A_{x_p} in **Eq. (9)** is obtained by doing the transformation in **Eq. (7)** where $R_{x,t}$ in this case is a matrix obtained by applying v_x basis functions to an exposure history vector $q_{x,t} = [x_p, x_p, x_p, \dots, x_p]^T$ whose elements are all equal to the same exposure level x_p. $\hat{\beta}_{x_p}$ can be interpreted as the risk level at each time step during the entire lag period resulted by exposure of level x_p at the current time step.

In the discussion section, relative risk is used to represent the risk contribution at each time lag. For DLNM, $\hat{\beta}_{x_p}$ in **Eq. (9)** are the parameters representing the risk level at each time step during the lag period. The relative risk is calculated as $\exp(\hat{\beta}_{x_p})$. For DLM the relative risk is calculated as $\exp(a\hat{\beta})$ where a is the number of units change in exposure intensity since $\hat{\beta}$ in **Eq. (5)** represents the risk contribution at each time lag brough by one unit change of exposure. Thus, relative risk greater than 1 means increasing segment crash risk, relative risk less than 1 means decreasing segment crash risk, and relative risk equal to 1 means no effect on the segment crash risk.

For the proposed analysis, a conditional Poisson approach is applied, and the quasi-Poisson distribution is assumed. **Eq. (10)** and **(11)** are the mathematical representations of the proposed quasi-Poisson model, where Y_t is the number of crashes of a specific roadway segment in a specific hour. $precp_{t,l}$ is the cross-basis matrix of hourly precipitation, $vsby_{t,l}$ is the cross-basis matrix of hourly visibility, $spdstd_{t,l}$ is the cross-basis matrix of hourly speed standard deviation, and $temp_{t,l}$ is the cross-basis matrix of hourly temperature. $\eta_1, \eta_2, \eta_3, \eta_4$ are the corresponding parameters vector with the parameters of the new variables created by the transformation.

$$E(Y_t) = \mu_t = \exp\left(\alpha + \eta_1 precp_{t,l} + \eta_2 vsby_{t,l} + \eta_3 spdstd_{t,l} + \eta_4 temp_{t,l}\right) \tag{10}$$

$$Y_t = poisson(\mu_t) \tag{11}$$

RESULTS AND DISCUSSIONS

A DLM model and a DLNM model (see **Table 3**) are fitted using the prepared dataset. For the DLM model, the exposure-response functions $f(x)$ for all four time-series variables are linear,

which means no transformations are performed to the exposure space. The lag-response functions $w(l)$ for all four time-series variables are B-spline function with 5 degrees of freedom. The total degree of freedom (v_l) of the cross-basis of all four time-series variables are 5. As for the DLNM model, the exposure-response functions $f(x)$ for all four time-series variables are polynomial. $f(x)$ of hourly precipitation has a degree of freedom (v_x) equal to 2, and $f(x)$ for other time-series variables has a degree of freedom (v_x) equal to 4. The lag-response functions $w(l)$ for hourly precipitation and hourly visibility are polynomial with degree of freedom (v_l) equal to 6 (5+Intercept), and the lag-response functions $w(l)$ for hourly speed standard deviation and hourly temperature are Natural cubic B-splines with degree of freedom (v_l) equal to 5. The cross-basis of hourly precipitation has degree of freedom ($v_x v_l$) equal to 12, the cross-basis of hourly visibility has degree of freedom ($v_x v_l$) equal to 24, and the cross-basis of hourly speed standard deviation and hourly temperature has degree of freedom ($v_x v_l$) equal to 20.

This study uses Akaike information criterion (AIC) scores to compare the performance of the DLM and the DLNM models. AIC scores were calculated using **Eq. (12).**

$$AIC = -2\ln(L) + 2k \tag{12}$$

Where L is the log-likelihood estimation of the model and k is the degree of freedom of the model. Note that for the quasi-Poisson model, the AIC score is also referred to as quasi-AIC (Bolker, 2017). The models with lower AIC scores were considered to have better performance than the ones with higher AIC scores. Based on the results, the DLM model's AIC score is 36241.98, and the DLNM model's AIC score is 35928.73. The two models have similar performances, but the DLNM model slightly overperforms the DLM model.

Table 3. DLM and DLNM models

DLM	$f(x)$	$f(x)$ df	$w(l)$	$w(l)$ df	$Total\ df$	AIC
Precip	Linear	1	B-splines	5	5	36241.98
Vsby	Linear	1	B-splines	5	5	
SpdStd	Linear	1	B-splines	5	5	
Temp	Linear	1	B-splines	5	5	
DLNM	$f(x)$	$f(x)$ df	$w(l)$	$w(l)$ df	$Total\ df$	AIC
Precip	Polynomials	2	Polynomials	5+Intercept	12	35928.73
Vsby	Polynomials	4	Polynomials	5+Intercept	24	
SpdStd	Polynomials	4	Natural cubic B-splines	5	20	
Temp	Polynomials	4	Natural cubic B-splines	5	20	

* Precip = hourly precipitation; Vsby = hourly visibility; SpdStd = hourly speed standard deviation; Temp = hourly temperature; df = degree of freedom

Hourly Precipitation

The modeling results of the exposure-lag-response association of hourly precipitation are presented in this section. **Table 4** presents the relative risk contribution at each lagged hour brought by hourly precipitation exposure, the numbers in the parentheses are the lower 95% confidence interval and the upper 95% confidence interval.

Table 4. Relative Risk at each Lag Hour Resulted by Precipitation Exposure

DLM

	Hourly Precipitation Intensity (Inches)					
Lagged hours	0.1	0.5	1	1.5	2	3
0	1(0.95,1.04)	0.98(0.77,1.24)	0.95(0.6,1.53)	0.93(0.46,1.89)	0.91(0.35,2.34)	0.87(0.21,3.58)
1	1.03(1.01,1.06)	1.19(1.07,1.31)	1.41(1.16,1.72)	1.67(1.24,2.25)	1.99(1.34,2.95)	2.8(1.54,5.08)
2	1.04(1.01,1.07)	1.21(1.06,1.37)	1.46(1.13,1.88)	1.77(1.21,2.59)	2.14(1.28,3.55)	3.12(1.45,6.7)
3	1.02(1.01,1.04)	1.12(1.04,1.21)	1.26(1.09,1.47)	1.42(1.13,1.78)	1.6(1.18,2.16)	2.02(1.29,3.18)
4	1.01(1,1.01)	1.04(1.01,1.07)	1.09(1.03,1.15)	1.13(1.04,1.23)	1.18(1.05,1.32)	1.28(1.08,1.52)
5	1(1,1.01)	1.02(1,1.05)	1.05(0.99,1.11)	1.08(0.99,1.17)	1.1(0.98,1.23)	1.16(0.98,1.37)
6	1.01(1,1.01)	1.04(1.01,1.07)	1.08(1.02,1.15)	1.13(1.02,1.24)	1.17(1.03,1.33)	1.27(1.05,1.53)
7	1.01(1,1.02)	1.04(0.99,1.08)	1.07(0.98,1.18)	1.11(0.97,1.28)	1.16(0.96,1.38)	1.24(0.95,1.63)
8	0.99(0.98,1.01)	0.96(0.9,1.03)	0.93(0.82,1.06)	0.9(0.74,1.09)	0.87(0.67,1.12)	0.81(0.54,1.19)

DLNM

	Hourly Precipitation Intensity (Inches)					
Lagged hours	0.1	0.5	1	1.5	2	3
0	1.05(0.94,1.17)	1.06(0.75,1.5)	0.73(0.37,1.46)	0.33(0.05,2.06)	0.1(0,4.14)	0(0,41.23)
1	1.08(1.01,1.16)	1.28(1,1.64)	1.11(0.68,1.79)	0.65(0.21,2.02)	0.26(0.03,2.45)	0.01(0,4.15)
2	1.05(1,1.1)	1.18(0.99,1.4)	1.16(0.83,1.63)	0.96(0.42,2.22)	0.67(0.12,3.59)	0.19(0,14.69)
3	1.02(0.99,1.06)	1.11(0.96,1.28)	1.18(0.89,1.56)	1.21(0.75,1.94)	1.19(0.56,2.54)	1.04(0.2,5.27)
4	1.02(0.99,1.05)	1.11(0.97,1.26)	1.22(0.95,1.58)	1.35(0.93,1.96)	1.48(0.91,2.42)	1.77(0.88,3.58)
5	1.02(0.99,1.05)	1.11(0.95,1.29)	1.22(0.91,1.65)	1.35(0.87,2.09)	1.48(0.84,2.61)	1.75(0.78,3.94)
6	1.01(0.98,1.04)	1.05(0.91,1.21)	1.1(0.84,1.44)	1.15(0.77,1.71)	1.2(0.72,2.02)	1.31(0.63,2.74)
7	1.01(0.96,1.06)	1.01(0.81,1.27)	0.93(0.59,1.46)	0.76(0.37,1.59)	0.57(0.18,1.74)	0.23(0.02,2.25)
8	1.13(1.02,1.26)	1.41(1.03,1.93)	0.99(0.53,1.86)	0.35(0.06,2)	0.06(0,2.3)	0(0,3.17)

*Numbers in the parentheses are: (lower 95% confidence interval, upper 95% confidence interval)

There is an obvious lagged impact on roadway crash risk brought by precipitation exposure according to the modelling results by both the DLM and DLNM models (see **Figure 2** and **Figure 3**). The results generated by DLM show that the instant impact of hourly precipitation on segment crash risk is minimal and the segment crash risk starts to increase and peaks at around 2 lagged hours after precipitation event happened. After around 2 lagged hours, the adverse impact on roadway crash risk brought by precipitation exposure then disappears. The results from previous studies show that hourly precipitation has instant impact on crash risk (Xing et al., 2019; Zhan et al., 2020), however, none of these studies use roadway segment based data to analyze the crash risk of each individual roadway segment. In this study, the results show that the instant impact of hourly precipitation on the crash risk of a roadway segment is small, and impact is lagged.

Furthermore, since DLNM also applies non-linear transformation on the exposure space, the results not only present the delayed impact of precipitation exposure, but more detailed information is also revealed by the DLNM. Firstly, lower hourly precipitation levels do not have apparent impact, neither positive nor negative, on segment crash risk at any lagged hour. As shown in **Figure 3**, the relative risk lines of hourly precipitation with levels of 0.1 inches and 0.5 inches are rather flat and very close to 1. This indicates that lower-level hourly precipitation exposure does not impact the segment crash risk too much at any lagged hour. Note that, the increases in relative risk at lag hour 8 of 0.1 inches and 0.5 hourly precipitation are likely caused by large confidence intervals and do not properly reflect the reality and the relative risk at lag hour 8 should be minimal as well. Secondly, for higher hourly precipitation levels (e.g. 1, 1.5, 2, and 3 inches per hour), the crash risk of a roadway segment is smaller than normal during the first few hours after high hourly precipitation happened (see **Figure 3**) which is to say, during the first few hours after high hourly precipitation happened, crashes are less likely to happen. This fact is likely because during the first few lagged hours after high hourly precipitation occur,

drivers tend to drive more safely by slowing down due to heavy rainfall. Previous studies also concluded that higher precipitation leads to safer driving behavior (Eisenberg, 2004; Wei et al., 2022b, 2022a). Although it is not obvious in **Figure 2**, this instant decrease in roadway crash risk brought by high-level hourly precipitation is also captured by the results of the DLM model. As shown in **Table 4**, the relative risk at lag hour 0 generated by the DLM model decreases as hourly precipitation intensity increases. Lastly, the lagged impact of higher levels hourly precipitation on segment crash risk starts to increase after the first few lagged hours and peaks at around lag hour 4 (see **Figure 3**). This is because after heavy rain stops, drivers on the roadway start to increase their driving speed while at the same time, the roadway surface becomes slippery due to the fact that rainfall accumulated on the roadway surface starts to mix with engine oil and gasoline accumulated on roadway surface under dry condition (Eisenberg, 2004). Slippery roadway surface and high driving speed together cause the segment crash risk to increase at the lagged hours.

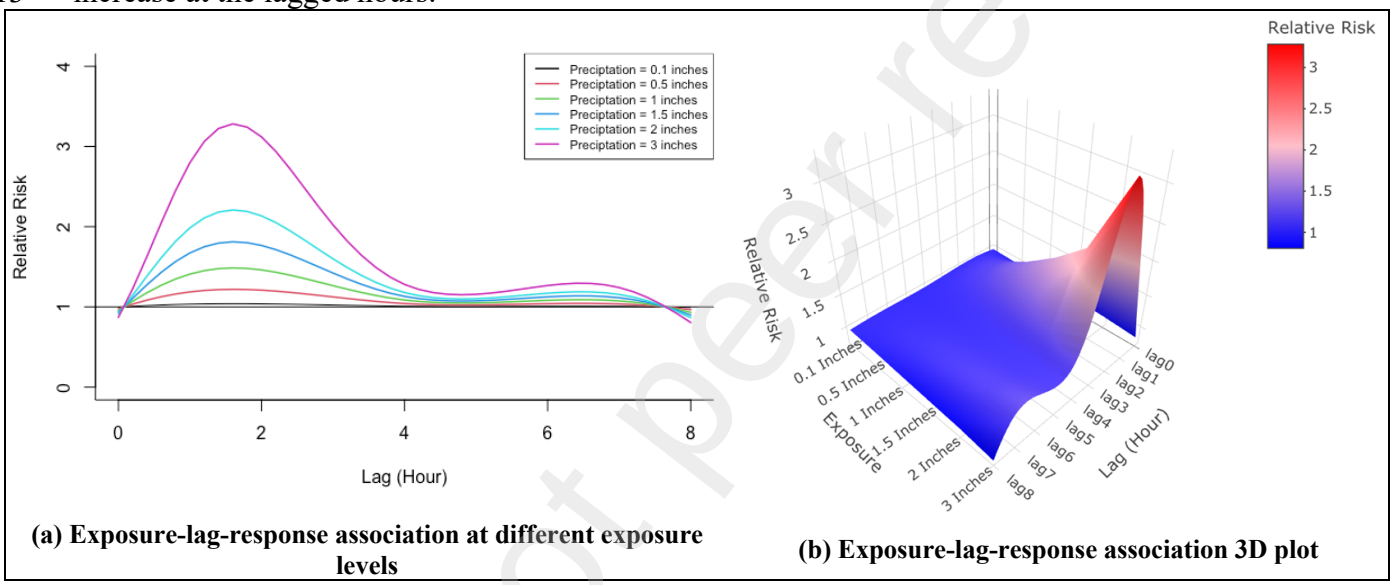

(a) Exposure-lag-response association at different exposure levels

(b) Exposure-lag-response association 3D plot

Figure 2. DLM exposure-lag-response association for hourly precipitation

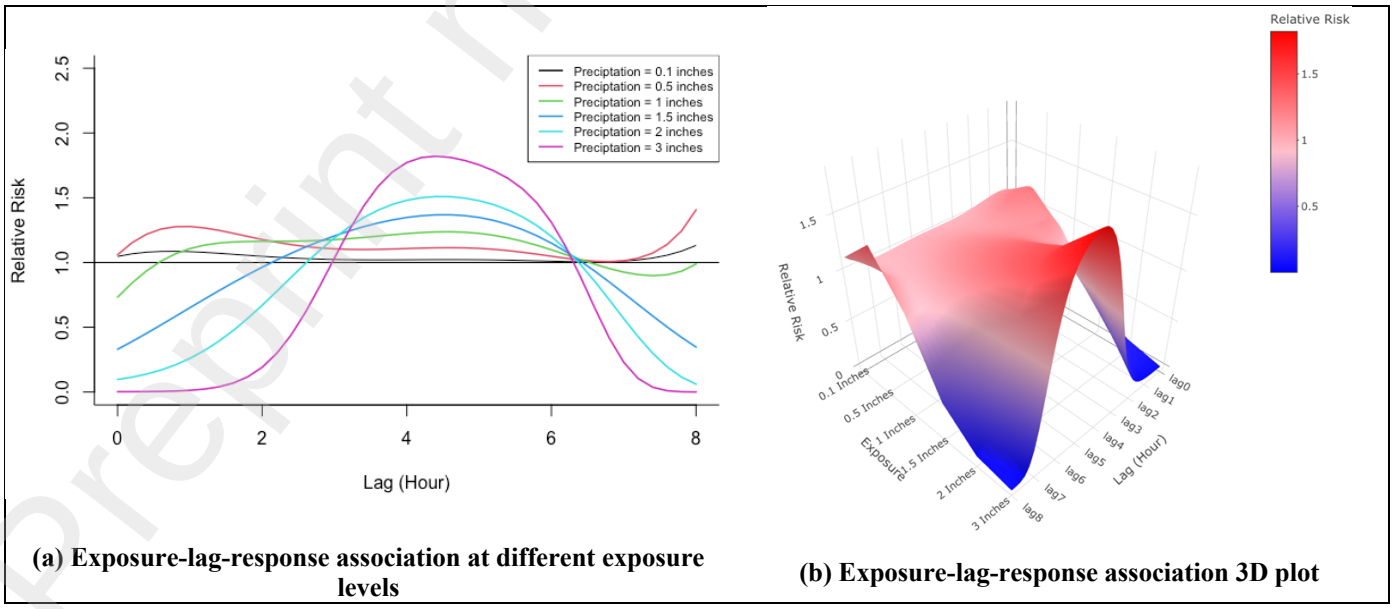

(a) Exposure-lag-response association at different exposure levels

(b) Exposure-lag-response association 3D plot

Figure 3. DLNM exposure-lag-response association for hourly precipitation

Both DLM and DLNM can reveal the lagged impact of hourly precipitation exposure on segment crash risk. Since the DLNM not only applies a non-linear transformation to the lagged space but also applies a non-linear transformation to the exposure space, it is capable of revealing more information on the exposure-lag-response association.

Note that the relative risk values shown in **Figure 2** and **Figure 3** represent the segment crash risk at each lagged hour brought by a 1-hour exposure at the current hour (lag hour 0). The exposure only occurs during the current hour and during the following lagged hours, there are no precipitation events happen. The relative risk value at lag hour l can be interpreted in two ways (forward and backward) as mentioned in the methodology section. First, it can be viewed as the exponential value of crash risk contribution at lag hour l resulting by the exposure at the current hour (lag hour 0). Meanwhile, it can also be viewed as the exponential value of crash risk contribution at the current hour (lag hour 0) resulting by the exposure at l hours beforehand. For continuous exposure that lasts for many hours, the cumulative impact on the segment crash risk should be accumulated by summing up the parameters $\hat{\beta}_{x_p}$ in **equation 9**. This fact applies to the other time-series variables in the following sections as well.

Hourly Visibility

The modeling results of the exposure-lag-response association of hourly visibility are presented in this section. **Table 5** presents the relative risk effects at each lagged hour brought by hourly visibility exposure.

Table 5. Relative Risk at each Lag Hour Resulted by Visibility Exposure

DLM						
	Hourly Visibility Level (Miles)					
Lagged hours	1	2	4	6	8	10
0	1.34(1.19,1.52)	1.3(1.17,1.45)	1.22(1.12,1.32)	1.14(1.08,1.2)	1.07(1.04,1.1)	1(1,1)
1	1.01(0.96,1.07)	1.01(0.96,1.06)	1.01(0.97,1.05)	1.01(0.98,1.03)	1(0.99,1.02)	1(1,1)
2	0.91(0.84,0.98)	0.92(0.85,0.98)	0.94(0.89,0.99)	0.96(0.92,0.99)	0.98(0.96,1)	1(1,1)
3	0.91(0.86,0.96)	0.92(0.87,0.96)	0.94(0.9,0.97)	0.96(0.94,0.98)	0.98(0.97,0.99)	1(1,1)
4	0.96(0.92,1.02)	0.97(0.93,1.01)	0.98(0.94,1.01)	0.98(0.96,1.01)	0.99(0.98,1)	1(1,1)
5	1.02(0.96,1.09)	1.02(0.96,1.08)	1.01(0.97,1.06)	1.01(0.98,1.04)	1(0.99,1.02)	1(1,1)
6	1.03(0.98,1.09)	1.03(0.98,1.08)	1.02(0.99,1.06)	1.01(0.99,1.04)	1.01(1,1.02)	1(1,1)
7	1.01(0.95,1.07)	1.01(0.96,1.06)	1.01(0.97,1.05)	1(0.98,1.03)	1(0.99,1.02)	1(1,1)
8	0.99(0.91,1.07)	0.99(0.92,1.06)	0.99(0.94,1.05)	0.99(0.96,1.03)	1(0.98,1.02)	1(1,1)
9	0.99(0.93,1.05)	0.99(0.94,1.04)	0.99(0.95,1.03)	0.99(0.97,1.02)	1(0.98,1.01)	1(1,1)
10	1.04(0.91,1.19)	1.04(0.92,1.17)	1.03(0.94,1.12)	1.02(0.96,1.08)	1.01(0.98,1.04)	1(1,1)
DLNM						
	Hourly Visibility Level (Miles)					
Lagged hours	1	2	4	6	8	10
0	1.46(1.22,1.74)	1.36(1.17,1.59)	1.26(1.12,1.41)	1.17(1.06,1.29)	1.07(0.98,1.17)	1(1,1)
1	0.87(0.76,1.01)	0.93(0.82,1.05)	0.99(0.9,1.08)	0.99(0.91,1.06)	0.97(0.9,1.03)	1(1,1)
2	0.84(0.76,0.93)	0.9(0.82,0.98)	0.97(0.91,1.04)	0.98(0.93,1.04)	0.97(0.92,1.02)	1(1,1)
3	0.94(0.86,1.03)	0.96(0.89,1.04)	1.01(0.95,1.07)	1.02(0.97,1.07)	1(0.95,1.04)	1(1,1)
4	1.03(0.94,1.13)	1.01(0.93,1.1)	1.01(0.96,1.08)	1.03(0.98,1.08)	1.02(0.98,1.07)	1(1,1)
5	1.05(0.97,1.13)	1.02(0.95,1.09)	0.99(0.94,1.04)	1.01(0.96,1.05)	1.03(0.99,1.07)	1(1,1)
6	1.02(0.92,1.12)	1(0.92,1.08)	0.96(0.91,1.02)	0.97(0.92,1.03)	1.01(0.97,1.06)	1(1,1)
7	0.98(0.9,1.08)	0.99(0.91,1.07)	0.97(0.92,1.03)	0.96(0.91,1.01)	0.98(0.94,1.03)	1(1,1)
8	0.99(0.89,1.11)	1.02(0.92,1.12)	1.02(0.95,1.09)	0.99(0.93,1.05)	0.96(0.91,1.01)	1(1,1)
9	1.03(0.89,1.2)	1.04(0.91,1.19)	1.06(0.97,1.17)	1.03(0.94,1.11)	0.96(0.9,1.03)	1(1,1)
10	1(0.82,1.22)	0.94(0.79,1.12)	0.96(0.84,1.09)	1(0.89,1.12)	1(0.91,1.1)	1(1,1)

*Numbers in the parentheses are: (lower 95% confidence interval, upper 95% confidence interval)

The patterns of the lagged impact of hourly visibility on segment crash risk obtained by DLM and DLNM are similar (see **Figure 4** and **Figure 5**). The instant impact on segment crash risk is very significant, and a lower visibility level brings a larger increase in segment crash risk. This finding echoes with some previous studies (Das et al., 2018; Peng et al., 2017). Moreover, the impact of low visibility drastically decreases at the following lagged hours. This indicates that the increase in segment crash risk brought by low visibility is instantaneous, and since visibility does not have the same kind of lagged impact as precipitation does once low visibility event ends, segment crash risk decreases quickly after the low visibility event ends.

However, one thing that is captured by the models is that during the first few hours after low visibility event happened (e.g., lag hours 1, 2, and 3), the relative crash risk decreases below 1 (see **Figure 4** and **Figure 5**). This indicates that a roadway segment is safer than normal during the first few hours after low visibility event happened. One possible explanation of this is that during the first few lag hours (e.g., lag hours 1, 2, and 3) after low visibility event happened, most of the drivers driving onto the roadway come from the roadways in the vicinity areas where at lag hour 0 (when low visibility happened) also have low visibility as well and these drivers are more likely to continue driving more cautiously.

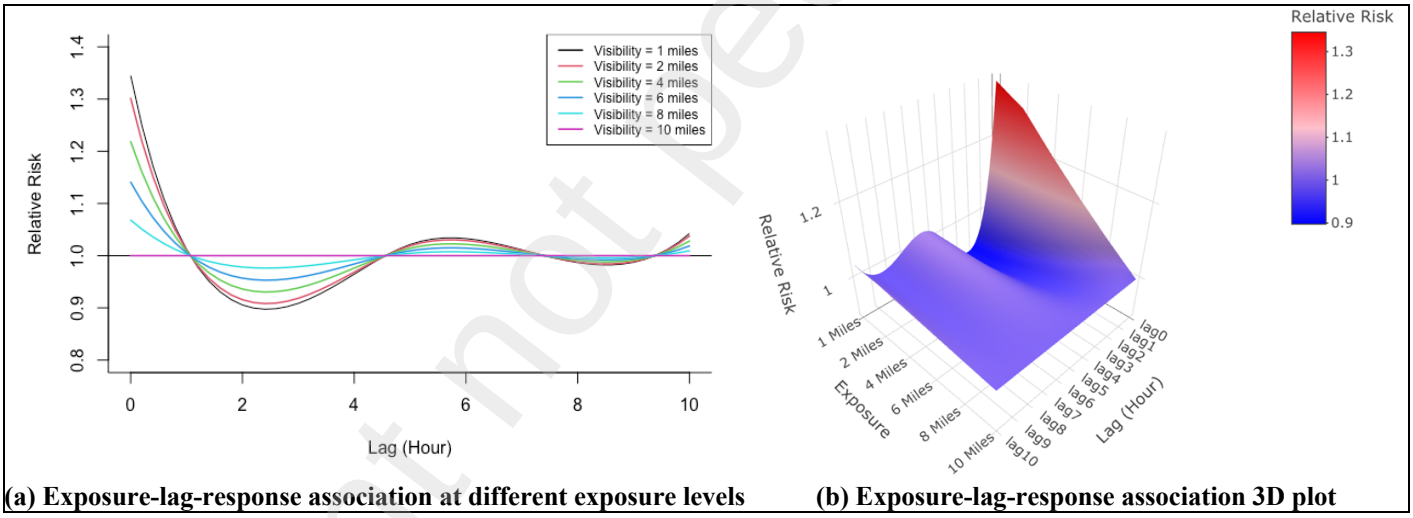

(a) Exposure-lag-response association at different exposure levels **(b) Exposure-lag-response association 3D plot**

Figure 4. DLM exposure-lag-response association for hourly visibility

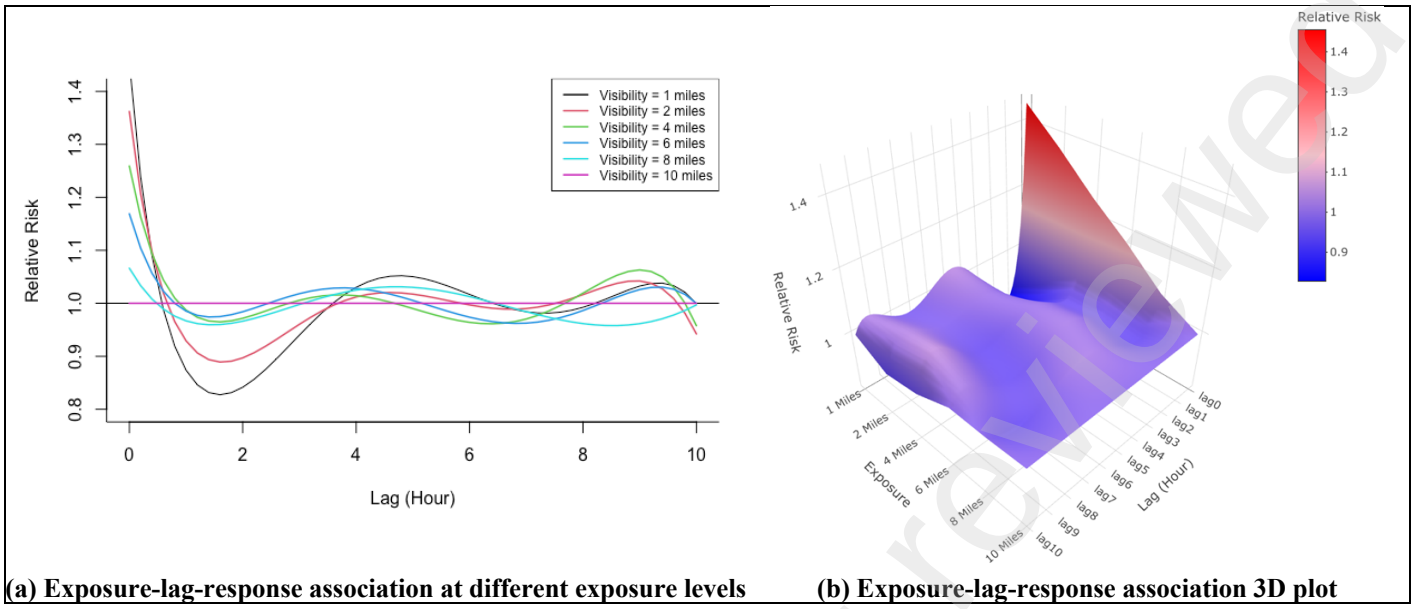

(a) Exposure-lag-response association at different exposure levels **(b) Exposure-lag-response association 3D plot**

Figure 5. DLNM exposure-lag-response association for hourly visibility

Hourly Temperature

The modeling results of the exposure-lag-response association of hourly temperature are presented in this section. **Table 6** presents the relative risk effects at each lag hour brought by hourly temperature exposure.

Table 6. Relative Risk at each Lag Hour Resulted by Temperature Exposure

DLM						
	Hourly Temperature Level (°F)					
Lagged hours	10	20	30	50	70	90
0	0.99(0.94,1.05)	0.98(0.88,1.11)	0.98(0.82,1.16)	0.96(0.72,1.29)	0.95(0.63,1.42)	0.93(0.55,1.57)
1	0.99(0.95,1.02)	0.97(0.91,1.04)	0.96(0.87,1.05)	0.93(0.79,1.09)	0.9(0.72,1.13)	0.88(0.66,1.17)
2	0.99(0.94,1.03)	0.98(0.89,1.07)	0.96(0.84,1.1)	0.94(0.75,1.18)	0.92(0.67,1.26)	0.89(0.59,1.35)
3	0.99(0.97,1.02)	0.99(0.94,1.04)	0.98(0.9,1.07)	0.97(0.85,1.12)	0.96(0.79,1.17)	0.95(0.74,1.22)
4	1(0.97,1.03)	1(0.95,1.06)	1.01(0.92,1.1)	1.01(0.88,1.17)	1.02(0.83,1.24)	1.02(0.79,1.32)
5	1.01(0.97,1.05)	1.02(0.94,1.11)	1.03(0.91,1.16)	1.04(0.85,1.29)	1.06(0.79,1.42)	1.08(0.74,1.57)
6	1.01(0.98,1.04)	1.02(0.96,1.08)	1.03(0.95,1.12)	1.05(0.91,1.21)	1.07(0.88,1.31)	1.1(0.85,1.41)
7	1.01(0.98,1.04)	1.02(0.96,1.08)	1.02(0.94,1.12)	1.04(0.9,1.21)	1.06(0.86,1.3)	1.08(0.82,1.41)
8	1(0.96,1.05)	1.01(0.92,1.11)	1.01(0.88,1.17)	1.02(0.81,1.3)	1.03(0.74,1.44)	1.04(0.68,1.6)
9	1(0.97,1.03)	1(0.94,1.07)	1.01(0.91,1.11)	1.01(0.86,1.19)	1.01(0.81,1.27)	1.02(0.76,1.36)
10	1(0.94,1.07)	1(0.88,1.14)	1(0.83,1.21)	1.01(0.74,1.38)	1.01(0.65,1.57)	1.01(0.58,1.78)
DLNM						
	Hourly Temperature Level (°F)					
Lagged hours	10	20	30	50	70	90
0	3.47(1.08,11.17)	1.55(0.94,2.57)	1.08(0.84,1.38)	0.97(0.9,1.05)	1(0.94,1.08)	0.97(0.8,1.17)
1	1.32(0.88,1.98)	1.17(0.98,1.39)	1.08(0.99,1.18)	1.01(0.98,1.03)	1(0.97,1.02)	0.96(0.9,1.03)
2	0.67(0.25,1.82)	0.94(0.6,1.45)	1.06(0.84,1.33)	1.03(0.96,1.1)	0.99(0.93,1.05)	0.96(0.81,1.15)
3	0.59(0.26,1.32)	0.85(0.6,1.22)	1(0.84,1.2)	1.03(0.97,1.09)	0.98(0.94,1.03)	0.97(0.84,1.11)
4	0.83(0.42,1.65)	0.88(0.65,1.19)	0.94(0.8,1.09)	1(0.96,1.05)	0.98(0.94,1.02)	0.98(0.88,1.1)
5	1.21(0.4,3.63)	0.95(0.58,1.55)	0.9(0.7,1.16)	0.98(0.91,1.05)	0.99(0.93,1.06)	1(0.82,1.21)
6	1.27(0.65,2.49)	1.01(0.75,1.36)	0.93(0.81,1.08)	0.97(0.93,1.01)	1.02(0.98,1.06)	1.03(0.92,1.15)
7	1.1(0.45,2.71)	1.05(0.7,1.56)	1(0.82,1.22)	0.97(0.92,1.03)	1.04(0.99,1.09)	1.06(0.91,1.22)
8	0.97(0.33,2.84)	1.06(0.66,1.7)	1.05(0.82,1.34)	0.99(0.92,1.06)	1.04(0.97,1.1)	1.06(0.89,1.27)
9	0.96(0.61,1.52)	1.04(0.86,1.27)	1.06(0.96,1.16)	1.01(0.99,1.04)	1(0.98,1.03)	1.04(0.97,1.12)
10	1(0.25,3.96)	1.02(0.56,1.84)	1.04(0.78,1.39)	1.04(0.96,1.13)	0.96(0.89,1.03)	1.01(0.82,1.25)

*Numbers in the parentheses are: (lower 95% confidence interval, upper 95% confidence interval)

The modeling results of DLM show that there is neither instant nor lagged impact on roadway crash risk by hourly temperature exposure (see **Figure 6**). The relative risk lines of all temperature levels are flat and close to 1. However, the results from DLNM model provide more information on the impact of hourly temperature exposure on roadway crash risk (see **Figure 7**). For higher temperature levels (e.g., 30°F, 50°F, 70°F, and 90°F), there is no obvious impact on roadway crash risk. This agrees with the results of the DLM model. While for lower temperature levels (e.g., 10°F and 20°F), the results from DLNM model show that there is an instant impact on roadway crash risk brought by low temperature exposure. Especially for 10°F and 20°F hourly temperature, there is a significant increase in roadway crash relative risk at lag hour 0. During the few hours after low temperature exposure happened, the crash relative risk decreases to below 1 and gradually returns to 1 afterward. This pattern is also seen in the modeling results of hourly visibility. The possible explanation for this pattern is that low temperature exposure is highly likely to cause moisture roadway surfaces to become icy, which can adversely increase segment crash risk. Moreover, during the first few hours right after low temperature exposure ends, most of the drivers driving on the roadway segment come from the roadway segments in vicinity areas and these drivers at lag hour 0 also experienced low temperature and have adapted more cautious driving behavior (Brijs et al., 2008). Thus, during the first few hours after low temperature exposure happened when they are driving on the current roadway segment, they are still driving in a cautious manner which makes the segment crash risk lower than normal.

The possible reason why the DLM model does not capture the impact of low hourly temperature on segment crash risk is in the following: Unlike other time-series variables analyzed in this study, since temperature is largely dependent on seasonality, in the dataset analyzed in this study, it is extremely rare to see hourly temperature changes a lot. For example, it is nearly impossible to see temperature changes from 10°F in the current hour to 80°F in the next hour. As a result, the DLM model is not able to generate any valuable results. The advantage of the DLNM model is that since it applies non-linear transformation onto the exposure space (in this study is polynomial transformation), a relatively small variation in hourly temperature can be magnified by the transformation. This potentially helps the model to find the instant and lagged impact of low hourly temperature on segment crash risk.

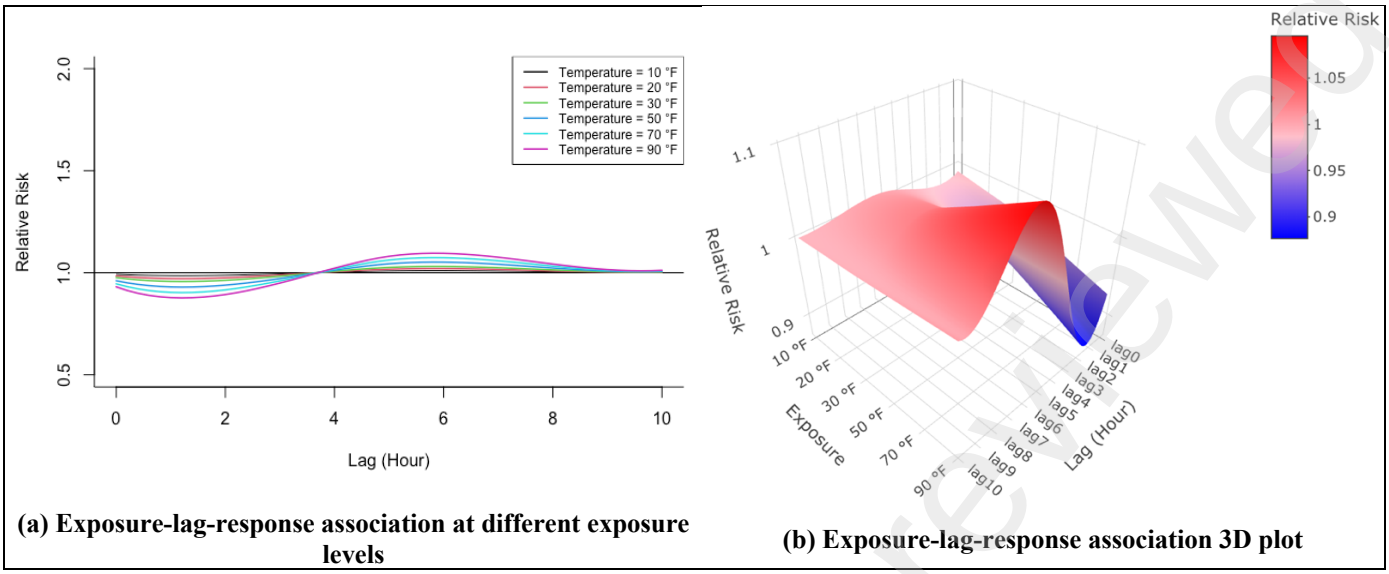

(a) Exposure-lag-response association at different exposure levels

(b) Exposure-lag-response association 3D plot

Figure 6. DLM exposure-lag-response association for hourly temperature

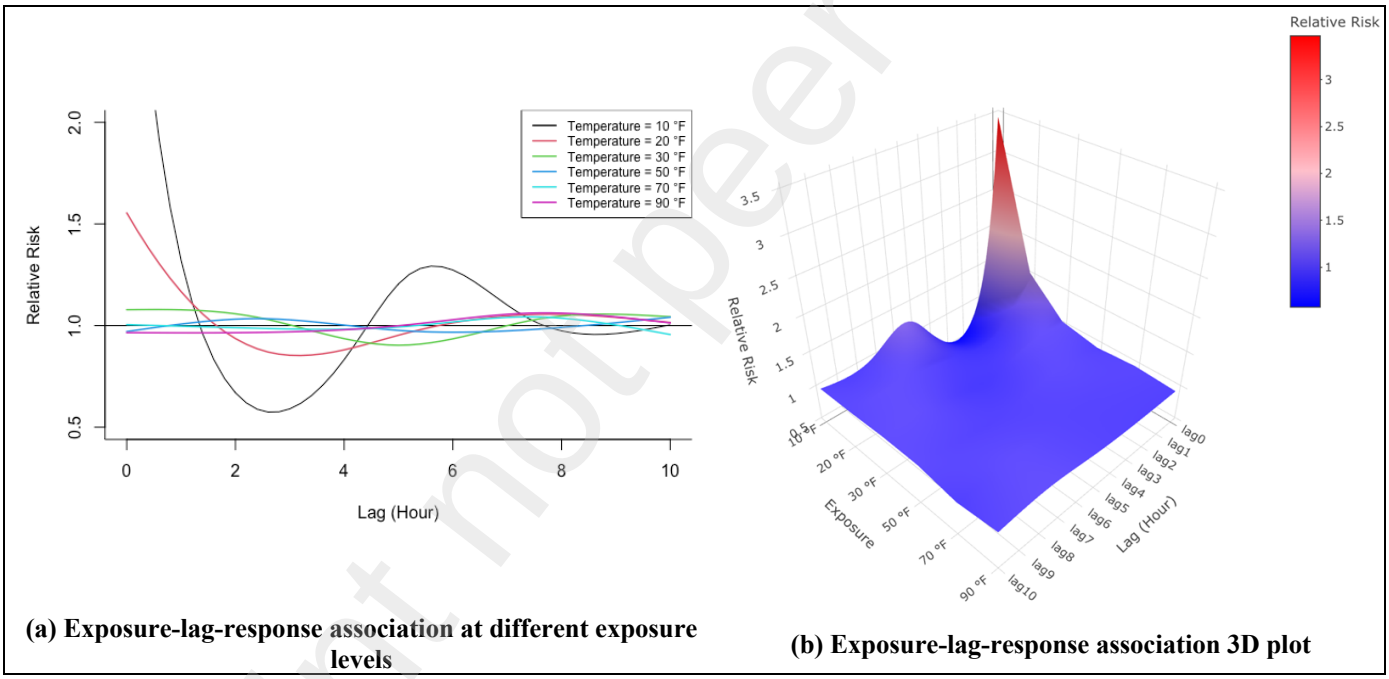

(a) Exposure-lag-response association at different exposure levels

(b) Exposure-lag-response association 3D plot

Figure 7. DLNM exposure-lag-response association for hourly temperature

Hourly Speed Standard Deviation

The modeling results of the exposure-lag-response association of hourly speed standard deviation are presented in this section. **Table 7** presents the relative risk effects at each lag hour brought by hourly speed standard deviation exposure.

Table 7. Relative Risk at each Lag Hour Resulted by Speed Standard Deviation Exposure

DLM

	Hourly Speed Standard Deviation Level (mph)					
Lagged hours	5	6	7	8	9	10

0	2.03(1.98,2.07)	2.33(2.27,2.4)	2.69(2.6,2.77)	3.09(2.98,3.21)	3.56(3.42,3.71)	4.1(3.92,4.3)
1	1.24(1.21,1.27)	1.3(1.26,1.34)	1.36(1.31,1.4)	1.42(1.36,1.47)	1.48(1.41,1.55)	1.54(1.47,1.62)
2	0.98(0.95,1)	0.97(0.94,1)	0.97(0.93,1)	0.96(0.92,1.01)	0.96(0.91,1.01)	0.95(0.9,1.01)
3	0.91(0.89,0.93)	0.89(0.87,0.92)	0.88(0.85,0.9)	0.86(0.83,0.89)	0.84(0.81,0.88)	0.83(0.79,0.87)
4	0.93(0.91,0.96)	0.92(0.89,0.95)	0.91(0.87,0.95)	0.9(0.86,0.94)	0.88(0.84,0.93)	0.87(0.82,0.92)
5	0.98(0.95,1.01)	0.98(0.94,1.01)	0.97(0.93,1.02)	0.97(0.92,1.02)	0.96(0.91,1.02)	0.96(0.9,1.02)
6	0.99(0.96,1.02)	0.99(0.96,1.02)	0.99(0.95,1.02)	0.98(0.94,1.03)	0.98(0.93,1.03)	0.98(0.93,1.03)
7	0.97(0.94,1)	0.96(0.93,1)	0.95(0.91,1)	0.95(0.9,1)	0.94(0.89,1)	0.94(0.88,1)
8	0.94(0.9,0.97)	0.92(0.88,0.97)	0.91(0.86,0.96)	0.9(0.84,0.96)	0.89(0.83,0.95)	0.87(0.81,0.95)
9	0.91(0.88,0.94)	0.9(0.86,0.93)	0.88(0.84,0.92)	0.86(0.82,0.91)	0.85(0.8,0.9)	0.83(0.78,0.89)
10	0.92(0.86,0.98)	0.9(0.84,0.98)	0.89(0.81,0.97)	0.87(0.79,0.97)	0.86(0.77,0.97)	0.85(0.74,0.96)

DLNM

	Hourly Speed Standard Deviation Level (mph)					
Lagged hours	5	6	7	8	9	10
0	3.87(3.28,4.57)	4.81(4.07,5.68)	5.83(4.95,6.86)	6.9(5.9,8.07)	7.96(6.85,9.25)	8.96(7.76,10.35)
1	1.61(1.46,1.77)	1.74(1.59,1.92)	1.88(1.71,2.05)	2(1.84,2.18)	2.12(1.95,2.31)	2.23(2.06,2.42)
2	0.84(0.73,0.95)	0.82(0.72,0.93)	0.81(0.71,0.91)	0.8(0.71,0.9)	0.79(0.71,0.89)	0.79(0.71,0.89)
3	0.67(0.6,0.75)	0.63(0.57,0.71)	0.61(0.54,0.68)	0.59(0.53,0.65)	0.57(0.52,0.64)	0.57(0.51,0.63)
4	0.79(0.71,0.89)	0.77(0.69,0.85)	0.75(0.68,0.83)	0.74(0.67,0.82)	0.74(0.67,0.81)	0.74(0.67,0.82)
5	1(0.86,1.15)	1(0.87,1.15)	1.01(0.88,1.15)	1.02(0.89,1.16)	1.04(0.91,1.18)	1.06(0.93,1.21)
6	1.04(0.93,1.17)	1.05(0.94,1.17)	1.06(0.95,1.17)	1.07(0.97,1.18)	1.08(0.98,1.19)	1.1(0.99,1.21)
7	0.96(0.84,1.1)	0.95(0.84,1.08)	0.94(0.84,1.06)	0.94(0.83,1.05)	0.93(0.83,1.04)	0.92(0.82,1.04)
8	0.88(0.76,1.02)	0.86(0.75,0.99)	0.85(0.74,0.96)	0.83(0.73,0.94)	0.82(0.72,0.93)	0.8(0.7,0.92)
9	0.85(0.76,0.94)	0.83(0.75,0.92)	0.82(0.74,0.9)	0.81(0.74,0.88)	0.8(0.73,0.87)	0.79(0.71,0.87)
10	0.84(0.69,1.03)	0.83(0.68,1.01)	0.82(0.68,0.99)	0.82(0.69,0.98)	0.82(0.69,0.98)	0.83(0.69,0.99)

*Numbers in the parentheses are: (lower 95% confidence interval, upper 95% confidence interval)

The results from both the DLM and DLNM models both show that there are some lagged impacts of high speed variation exposure on segment crash risk (see **Figure 8** and **Figure 9**) but the lagged impact does not exist long. The instant impact on roadway crash risk at lag hour 0 is significant and it quickly disappears in the lagged hours after high speed variation exposure happened. From **Figure 8** and **Figure 9**, it can be seen that after around 1 hour after high speed variation exposure happened, there are no longer obvious lagged impacts. This is because speed variation is not always consistent on segments closed to each other, drivers driving on one roadway segment during the lagged hours after high speed variation happened did not experience high speed variation at lag hour 0 since they were driving on other roadway segments in vicinity areas where do share the same level of speed variation. Note that the results from DLM and DLNM show a similar exposure-lag-response association, while the DLNM model tends to estimate a higher relative risk level at each lag hour than the DLM model. This is likely due to the polynomial transformation applied on the exposure space in the DLNM model.

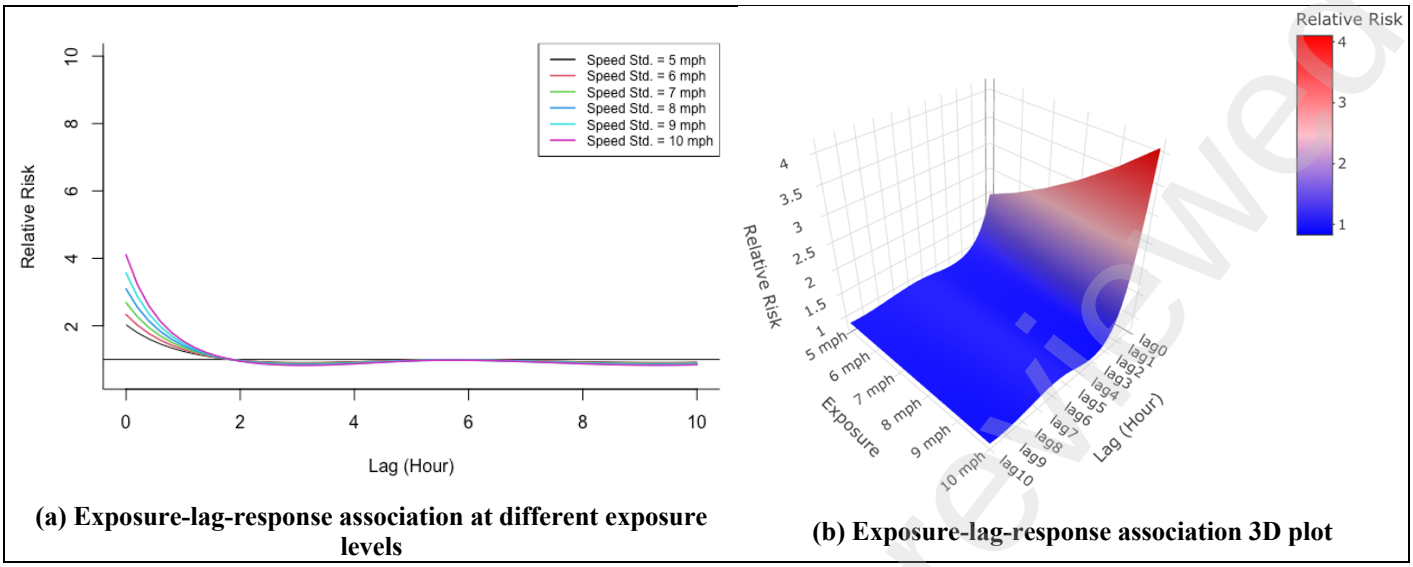

(a) Exposure-lag-response association at different exposure levels

(b) Exposure-lag-response association 3D plot

Figure 8. DLM exposure-lag-response association for hourly speed standard deviation

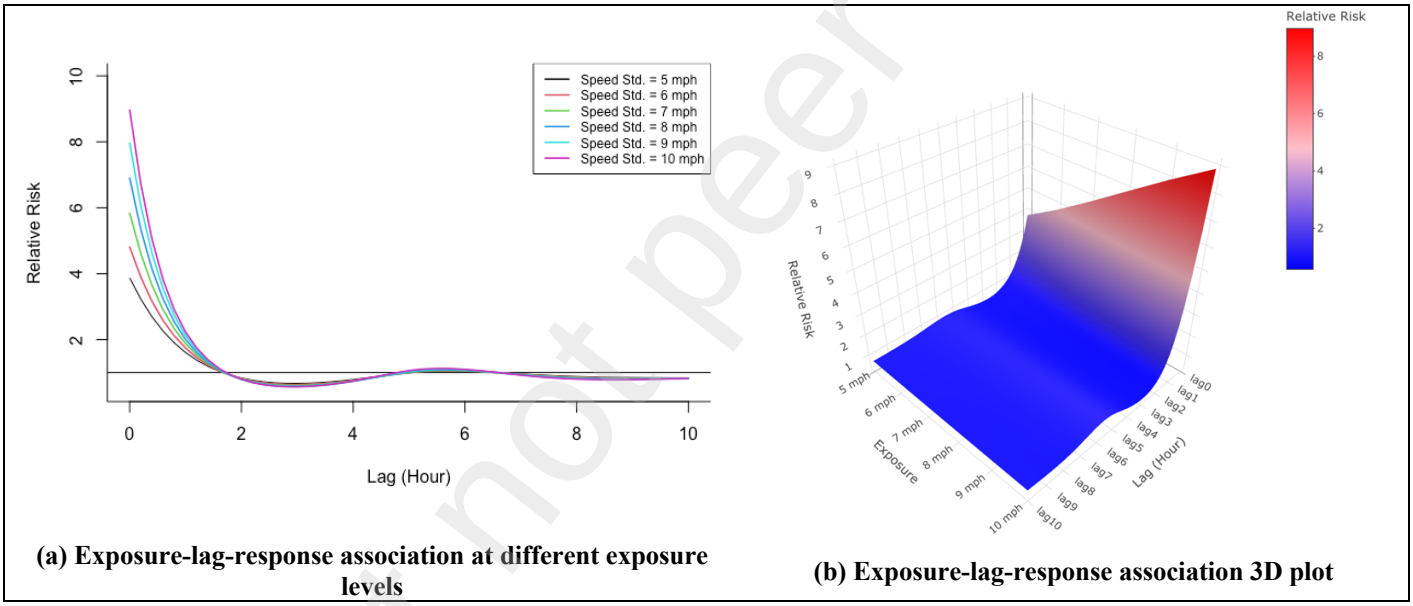

(a) Exposure-lag-response association at different exposure levels

(b) Exposure-lag-response association 3D plot

Figure 9. DLNM exposure-lag-response association for hourly speed standard deviation

CONCLUSIONS

Weather factors and speed variation factors are closely related to the crash risk of a roadway segment. Methods in previous studies often assume crashes to be only related to the weather and speed variation events that occurred during the same time period and uses data with large aggregation interval. In reality, weather and high speed variation events not only have impacts on segment crash risk during the same period as the events happen, but also have a lasting impact on segment crash risk during the lagged time periods after the events occurred. The lagged impacts of weather factors and speed variation factors on segment crash risk are rarely studied previously. In order to fill this research gap, this study applies a distributed lag model (DLM) and a distributed lag nonlinear model (DLNM) to investigate the exposure-lag-response association between segment crash risk and four time-series variables: hourly precipitation,

hourly visibility, hourly speed standard deviation, and hourly temperature. The segment crash risk is represented by the number of crashes that happen on a particular roadway segment during a 1-hour period.

The results show that for some time-series variables such as hourly precipitation and hourly temperature, DLNM can capture more information of the exposure-lag-response association compared with DLM since DLNM applies non-linear transformation on the exposure space. For each time-series variable, the results of DLM and DLNM demonstrate that the instant impact of hourly precipitation event is very small at the current hour. The impact in segment crash risk increases and starts to peak during the first few lagged hours after hourly precipitation event happened. Moreover, at the current hour, higher hourly precipitation intensity makes segment crash risk lower than that of lower hourly precipitation intensity because higher precipitation intensity makes drivers drive more cautiously. While at the lagged hour when segment crash risk peaks, higher hourly precipitation intensity still brings higher peaked risk than lower hourly precipitation intensity. As for hourly visibility exposure, both the DLM and DLNM model show similar results. Low visibility event poses a significant impact on segment crash risk at the current hour. The results also show that during the first few lagged hours after low visibility occurred, the roadway is safer than normal. For hourly temperature exposure, the results from DLM do not show obvious impact of temperature factor on segment crash risk. While since DLNM applies non-linear transformation to the exposure space, the DLNM model reveals that although the higher hourly temperature does not have obvious impact on segment crash risk, lower hourly temperature poses a significant impact on segment crash risk at the current hour, and it also has lagged impact. The relative risk at the current hour is 3.47 under 10 °F hourly temperature, and for 20 °F the relative risk at the current hour is 1.55. Finally, for hourly speed standard deviation exposure, both the DLM and DLNM models show significant relative risk at the current hour. While there is no obvious lagged impact, the relative risk quickly decreases to one after high speed standard deviation event happens.

The results of this study describe the impact of weather and speed variation events on segment crash risk in a more accurate and comprehensive way. The impact is not only considered at the current hour but also at the lagged hours. Since the lagged impacts are still considerable after the presence of extreme weather or speed variation events, it is needed to design weather and crash warning systems to inform roadway users the potential increases in crash risk in advance. Moreover, from the perspective of allocating first respondent resources, it is possible to let the decision maker identify the potential crash hotpots in real time after severe weather and high speed variation events occur. Future studies can further explore the exposure-lag-response association between these time-series variables and roadway crash risk on different roadway facility types other than rural interstate highways. Crash severity should also be considered in future studies. Moreover, the impact of non-time-series variables, such as geometric information on the exposure-lag-response association, can also be further investigated.

REFERENCES

Anderson, I.B., Bauer, K.M., Harwood, D.W., Fitzpatrick, K., 1999. Relationship to Safety of Geometric Design Consistency Measures for Rural Two-Lane Highways. Transportation Research Record 1658, 43–51. https://doi.org/10.3141/1658-06

Andrey, J., Yagar, S., 1993. A temporal analysis of rain-related crash risk. Accident Analysis & Prevention 25, 465–472. https://doi.org/10.1016/0001-4575(93)90076-9
Bolker, B., 2017. Dealing with quasi- models in R.
Brijs, T., Karlis, D., Wets, G., 2008. Studying the effect of weather conditions on daily crash counts using a discrete time-series model. Accident Analysis & Prevention 40, 1180–1190. https://doi.org/10.1016/j.aap.2008.01.001
Das, S., Brimley, B.K., Lindheimer, T.E., Zupancich, M., 2018. Association of reduced visibility with crash outcomes. IATSS Research 42, 143–151. https://doi.org/10.1016/j.iatssr.2017.10.003
Das, S., Geedipally, S., Avelar, R., Wu, L., Fitzpatrick, K., Banihashemi, M., Lord, D., 2020. Rural Speed Safety Project for USDOT Safety Data Initiative.
Das, S., Geedipally, S., Fitzpatrick, K., Park, E., Wu, L., Wei, Z., Tsapakis, I., Paal, S., 2022a. Develop a Real-Time Decision Support Tool for Rural Roadway Safety Improvements. TxDOT, Austin, TX.
Das, S., Geedipally, S.R., Fitzpatrick, K., 2021. Inclusion of speed and weather measures in safety performance functions for rural roadways. IATSS Research 45, 60–69. https://doi.org/10.1016/j.iatssr.2020.05.001
Das, S., Le, M., Fitzpatrick, K., Wu, D., 2022b. Did Operating Speeds During COVID-19 Result in More Fatal and Injury Crashes on Urban Freeways? Transportation Research Record 03611981221109597. https://doi.org/10.1177/03611981221109597
Das, S., White, L.D., 2020. RuralSpeedSafetyX: Interactive decision support tool to improve safety. SoftwareX 11, 100493. https://doi.org/10.1016/j.softx.2020.100493
Dutta, N., Fontaine, M.D., 2019. Improving freeway segment crash prediction models by including disaggregate speed data from different sources. Accident Analysis & Prevention 132, 105253. https://doi.org/10.1016/j.aap.2019.07.029
Eisenberg, D., 2004. The mixed effects of precipitation on traffic crashes. Accident Analysis & Prevention 36, 637–647. https://doi.org/10.1016/S0001-4575(03)00085-X
Ferreira Braga, A.L., Zanobetti, A., Schwartz, J., 2001. The Time Course of Weather-Related Deaths. Epidemiology 12, 662–667.
Gao, X., Jiang, W., Liao, J., Li, J., Yang, L., 2022. Attributable risk and economic cost of hospital admissions for depression due to short-exposure to ambient air pollution: A multi-city time-stratified case-crossover study. Journal of Affective Disorders 304, 150–158. https://doi.org/10.1016/j.jad.2022.02.064
Garber, N.J., Gadiraju, R., 1989. Factors affecting speed variance and its influence on accidents. Transportation research record 1213, 64–71.
Gasparrini, A., 2014. Modeling exposure-lag-response associations with distributed lag non-linear models. Stat Med 33, 881–899. https://doi.org/10.1002/sim.5963
Gasparrini, A., Armstrong, B., Kenward, M.G., 2010. Distributed lag non-linear models. Stat Med 29, 2224–2234. https://doi.org/10.1002/sim.3940
Guo, Y., Barnett, A.G., Pan, X., Yu, W., Tong, S., 2011. The Impact of Temperature on Mortality in Tianjin, China: A Case-Crossover Design with a Distributed Lag Nonlinear Model. Environmental Health Perspectives 119, 1719–1725. https://doi.org/10.1289/ehp.1103598
Haghighi, N., Liu, X.C., Zhang, G., Porter, R.J., 2018. Impact of roadway geometric features on crash severity on rural two-lane highways. Accident Analysis & Prevention 111, 34–42. https://doi.org/10.1016/j.aap.2017.11.014

Jaroszweski, D., McNamara, T., 2014. The influence of rainfall on road accidents in urban areas: A weather radar approach. Travel Behaviour and Society, Advances in Spatiotemporal Transport Analysis 1, 15–21. https://doi.org/10.1016/j.tbs.2013.10.005

Lee, C., Saccomanno, F., Hellinga, B., 2002. Analysis of Crash Precursors on Instrumented Freeways. Transportation Research Record 1784, 1–8. https://doi.org/10.3141/1784-01

Lord, D., Mannering, F., 2010. The statistical analysis of crash-frequency data: A review and assessment of methodological alternatives. Transportation Research Part A: Policy and Practice 44, 291–305. https://doi.org/10.1016/j.tra.2010.02.001

McCourt, R., Fitzpatrick, K., Koonce, P., Das, S., 2019. Speed Limits: Leading to Change. ITE Journal 89.

Miaou, S.-P., Lum, H., 1993. Modeling vehicle accidents and highway geometric design relationships. Accident Analysis & Prevention 25, 689–709. https://doi.org/10.1016/0001-4575(93)90034-T

National Center for Statistics and Analysis, 2022. Early Estimates of Motor Vehicle Traffic Fatalities and Fatality Rate by Sub-Categories 2021 (Crash•Stats Brief Statistical Summary. Report No. DOT HS 813 298). National Highway Traffic Safety Administration.

Nyadanu, S.D., Tessema, G.A., Mullins, B., Pereira, G., 2022. Maternal acute thermophysiological stress and stillbirth in Western Australia, 2000–2015: A space-time-stratified case-crossover analysis. Science of The Total Environment 836, 155750. https://doi.org/10.1016/j.scitotenv.2022.155750

Omranian, E., Sharif, H., Dessouky, S., Weissmann, J., 2018. Exploring rainfall impacts on the crash risk on Texas roadways: A crash-based matched-pairs analysis approach. Accident Analysis & Prevention 117, 10–20. https://doi.org/10.1016/j.aap.2018.03.030

Park, E.S., Fitzpatrick, K., Das, S., Avelar, R., 2021. Exploration of the relationship among roadway characteristics, operating speed, and crashes for city streets using path analysis. Accident Analysis & Prevention 150, 105896. https://doi.org/10.1016/j.aap.2020.105896

Pei, X., Wong, S.C., Sze, N.N., 2012. The roles of exposure and speed in road safety analysis. Accident Analysis & Prevention, Intelligent Speed Adaptation + Construction Projects 48, 464–471. https://doi.org/10.1016/j.aap.2012.03.005

Peng, Y., Abdel-Aty, M., Shi, Q., Yu, R., 2017. Assessing the impact of reduced visibility on traffic crash risk using microscopic data and surrogate safety measures. Transportation Research Part C: Emerging Technologies 74, 295–305. https://doi.org/10.1016/j.trc.2016.11.022

Schwartz, J., 2000. The Distributed Lag between Air Pollution and Daily Deaths. Epidemiology 11, 320–326.

Scott, P.P., 1986. Modelling time-series of British road accident data. Accident Analysis & Prevention, Special Issue Accident Modelling 18, 109–117. https://doi.org/10.1016/0001-4575(86)90055-2

Shankar, V., Mannering, F., Barfield, W., 1995. Effect of roadway geometrics and environmental factors on rural freeway accident frequencies. Accident Analysis & Prevention 27, 371–389. https://doi.org/10.1016/0001-4575(94)00078-Z

Texas Department of Transportation, 2020. Roadway Inventory [WWW Document]. URL https://www.txdot.gov/inside-txdot/division/transportation-planning/roadway-inventory.html (accessed 2.23.21).

Wang, X., Zhou, Q., Quddus, M., Fan, T., Fang, S., 2018. Speed, speed variation and crash relationships for urban arterials. Accident Analysis & Prevention 113, 236–243. https://doi.org/10.1016/j.aap.2018.01.032

Wei, Z., Das, S., Zhang, Y., 2022a. Short Duration Crash Prediction for Rural Two-Lane Roadways: Applying Explainable Artificial Intelligence. Transportation Research Record 03611981221096113. https://doi.org/10.1177/03611981221096113

Wei, Z., Zhang, Y., Das, S., 2022b. Applying Explainable Machine Learning Techniques in Daily Crash Occurrence and Severity Modeling for Rural Interstates. Transportation Research Record 03611981221134629. https://doi.org/10.1177/03611981221134629

Wu, Y., Li, S., Guo, Y., 2021. Space-Time-Stratified Case-Crossover Design in Environmental Epidemiology Study. Health Data Science 2021. https://doi.org/10.34133/2021/9870798

Xing, F., Huang, H., Zhan, Z., Zhai, X., Ou, C., Sze, N.N., Hon, K.K., 2019. Hourly associations between weather factors and traffic crashes: Non-linear and lag effects. Analytic Methods in Accident Research 24, 100109.

Yu, R., Abdel-Aty, M., 2014. Analyzing crash injury severity for a mountainous freeway incorporating real-time traffic and weather data. Safety Science 63, 50–56. https://doi.org/10.1016/j.ssci.2013.10.012

Zanobetti, A., Wand, M.P., Schwartz, J., Ryan, L.M., 2000. Generalized additive distributed lag models: quantifying mortality displacement. Biostatistics 1, 279–292. https://doi.org/10.1093/biostatistics/1.3.279

Zhan, Z.-Y., Yu, Y.-M., Chen, T.-T., Xu, L.-J., Ou, C.-Q., 2020. Effects of hourly precipitation and temperature on road traffic casualties in Shenzhen, China (2010–2016): A time-stratified case-crossover study. Science of The Total Environment 720, 137482. https://doi.org/10.1016/j.scitotenv.2020.137482